Inorganic Chemistry

Article

pubs.acs.org/IC

# Stereoselective Alkali-Metal Catalysts for Highly Isotactic Poly(*rac*-lactide) Synthesis

Yangyang Sun, Jiao Xiong, Zhongran Dai, Xiaobo Pan, Ning Tang, and Jincai Wu*

State Key Laboratory of Applied Organic Chemistry, College of Chemistry and Chemical Engineering, Key Laboratory of Nonferrous Metal Chemistry and Resources Utilization of Gansu Province, Lanzhou University, Lanzhou 730000, People's Republic of China

Supporting Information

**ABSTRACT:** A high degree of chain end control in the isoselective ring-opening polymerization (ROP) of *rac*-lactide is a challenging research goal. In this work, eight highly active sodium and potassium phenolates as highly isoselective catalysts for the ROP of *rac*-lactide are reported. The best isoselectivity value of $P_m$ = 0.94 is achieved. The isoselective mechanism is chain-end control through the analysis of the stereoerrors in the microstructure of a final polymer; thus, isotactic multiblock structure polymers are obtained, and the highest melt point can reach 192.5 °C. The donating group in phenolate can clearly accelerate the ROP reaction, potassium complexes are more active than the analogous sodium complexes, and the big spacial hindrance of the ligand can decrease the activity. The high isoselectivities of these complexes mostly result from their sandwich structure constructed by the plane of the crown and the plane of the anthryl group.

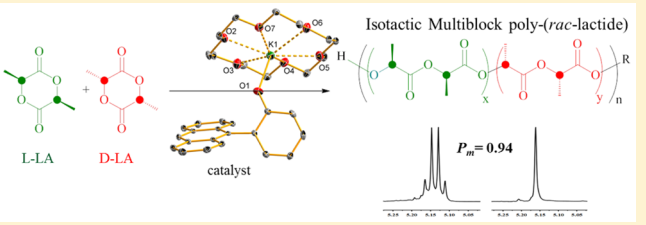


## INTRODUCTION

Stereoselective polymerization of chiral and prochiral monomers is a valuable research subject because different tactic polymers will own different chemical and physical characters.[1] Obviously, catalysts play a key role in this area, among which a metal catalyst with a suitable ligand is very attractive for the high efficiency, high selectivity, and easy tuning of the ligand.[2] Despite the fact that many stereoselective metal catalysts have been reported, sodium and potassium complexes as stereoselective catalysts with the real active center exclusively on the sodium or potassium ions have not been well developed. In the 1980s, Donald J. Cram et al. reported that several chiral crown ether potassium complexes can catalyze Michael addition reactions with high asymmetric induction and the polymerization of methacrylate esters, giving isotactic polymers,[3] which changed our bias on the ability of sodium and potassium complexes in stereoselective reactions and encouraged us to explore more stereoselective sodium or potassium metal complexes as catalysts for polymerization reactions or organic reactions.

Herein we extend the application of sodium/potassium complexes to the stereoselective synthesis of polylactide (PLA), because polylactide is an important bioderived polymer in wide fields such as packaging, fiber technology, and medicine.[4] As we know, the physical and chemical properties of polylactide highly associate with its stereoregularity. The stereocontrolled ring-opening polymerization (ROP) of *rac*-lactide is still a valuable and challenging research goal.[5] Especially, the isoselective ROP of *rac*-lactide needs to be explored further because some problems have not been overcome. For example, the excellent isoselective aluminum−Salen or aluminum−Salan initiators suffer from their low activities.[6] The isoselectivities of new emerging systems, such as yttrium phosphasalen alkoxides,[7] zinc amidooxazolinates,[8] and other complexes,[9] need to be improved further.

Sodium and potassium are nontoxic and cheap elements, and are suitable for the catalytic synthesis of polylactides,[10] especially in medical-related fields. Recently, we discovered that several sodium and potassium phenolate crown ether complexes can stereoselectively catalyze the ROP of *rac*-lactide, giving isotactic polylactide (**A**−**C** in Chart 1).[11] However, compared with the highly isoselective aluminum−Salen or aluminum−Salan system, the isoselectivities are not very high. Thus, in this work we try to improve the sodium/potassium phenolate crown ether system further with an attempt to get better isotacticities. We also want to understand this good system in detail via the study of the structure factors and reaction mechanism.

## RESULTS AND DISCUSSION

**Synthesis and Structures of Sandwich-Type Alkali-Metal Phenolates 1−8.** Our previous results show the bent xanthenyl plane of the *ortho* position in the phenol ligand is important for the isoselectivity of the ROP of *rac*-lactide (**A**−**C** in Chart 1).[11] Here, we changed the previous bent xanthenyl plane to a standard planar substituted group of anthryl (**D** in Chart 1, Scheme 1) to adjust the subtle confined space between the plane of the crown and the plane of the substituted group of phenol; a stronger interaction between the monomer and the

Received: August 27, 2015

  

DOI: 10.1021/acs.inorgchem.5b02709
*Inorg. Chem.* XXXX, XXX, XXX−XXX

**Chart 1. Alkali-Metal Crown Ether Complexes**[a]

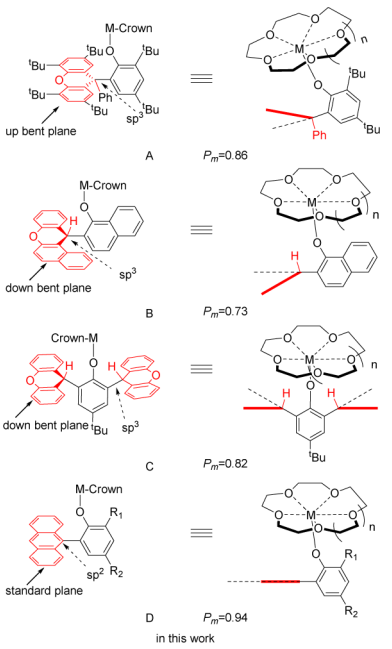


[a]The planar xanthenyl/anthryl groups are replaced with red lines in the right molecular structures to present their different extended orientations. Crown = 15-crown-5 or 18-crown-6. M = K or Na.

**Scheme 1. Synthesis of Complexes 1−8**

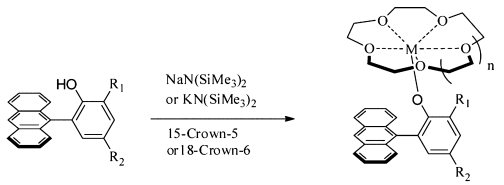


$H^1L$ $R_1$=H $R_2$=H
$H^2L$ $R_1$=H $R_2$=$^t$Bu
$H^3L$ $R_1$=H $R_2$=OMe
$H^4L$ $R_1$=$^t$Bu $R_2$=$^t$Bu

**1** M=K, n=2 $R_1$=H $R_2$=H
**2** M=K, n=2 $R_1$=H $R_2$=$^t$Bu
**3** M=K, n=2 $R_1$=H $R_2$=OMe
**4** M=K, n=2 $R_1$=$^t$Bu $R_2$=$^t$Bu
**5** M=Na, n=1 $R_1$=H $R_2$=H
**6** M=Na, n=1 $R_1$=H $R_2$=$^t$Bu
**7** M=Na, n=1 $R_1$=H $R_2$=OMe
**8** M=Na, n=1 $R_1$=$^t$Bu $R_2$=$^t$Bu

active end of the polymer chain can be expected in this special confined space. Four phenol ligands, $H^1L$−$H^4L$, were synthesized according to a literature method.[12] Complexes **1**−**8** were obtained in high yields via the reactions of the corresponding ligand with a stoichiometric amount of 18-crown-6/15-crown-5 and $KN(SiMe_3)_2$/$NaN(SiMe_3)_2$ in THF (Scheme 1). Crystals of complexes **1**, **3**, **4**, and **8** suitable for single-crystal X-ray diffraction were isolated from toluene, bezene, or glycol dimethyl ether solutions. Their molecular structures are shown in Figure 1. Compared to complex **1**, O1 of the phenoxy anion in complexes **3** and **4** is more negatively charged due to the electronic-donating ability of the methoxy group and two *tert*-butyl groups, which can give rise to a stronger interaction between K1 and O1. Thus, the K1−O1 bond distances of 2.444(5) Å in complex **3** and 2.498(2) Å in complex **4** are shorter than that of 2.5737(18) Å in complex **1**. Despite the repulsion between the crown ether and *tert*-butyl group at the *ortho* position, the K1−O1 bond in complex **4** is still shorter than that in complex **1**, which indicates the K1−O1 bond is affected significantly by the electronic nature of the

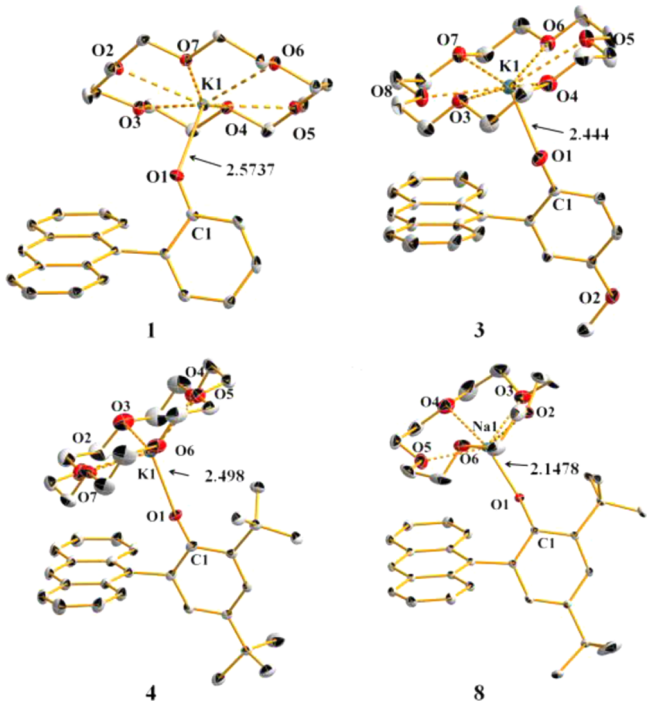


**Figure 1.** Molecular structures of **1**, **3**, **4**, and **8** with probability ellipsoids at 30% (all of the hydrogen atoms are omitted for clarity). Selected bond lengths (Å): complex **1**, K1−O1 = 2.5737(18), C1−O1 = 1.289(3); complex **3**, K1−O1 = 2.444(5), C1−O1 = 1.289(6); complex **4**, K1−O1 = 2.498(2), C1−O1 = 1.290(4); complex **8**, Na1−O1 = 2.1478(18), C1−O1 = 1.287(3).

substituent group. The Na1−O1 bond distance of 2.1478(18) Å in sodium analogue **8** is shorter than the K1−O1 bond distance of 2.498(2) Å in complex **4**. The four crystal structures demonstrate a very important feature of these complexes, that all $K^+$/$Na^+$ active centers are partially sandwiched between the plane of the crown ether and the plane of the anthryl group. Comparatively, the surroundings of the active K1 center of complexes **1**−**4** are less bulky than that in the potassium complex of **A** and more crowded than that in the potassium complexes of **B** and **C** due to the different extended orientation of the substituted planar group (Chart 1).[11] As we know, the catalytic activity and stereoselectivity are sensitive to the environment of the active center. The visually different distances of K1/Na1−O1 and spacial orientations of the crown ether and planar anthryl group may lead to different catalytic behaviors in the ROP of *rac*-lactide.

**Controllability of the ROP of *rac*-Lactide and Structure Influences of the Catalysts.** Complex **1** is a highly active catalyst for the polymerization of *rac*-lactide because the polymerization with a 100/1/1 $[rac\text{-LA}]_0/[\mathbf{1}]_0/[\text{BnOH}]_0$ ratio can be accomplished in 93% conversion within 2 min at room temperature in 5 mL of toluene (Table 1, entry 2, $[\text{cat.}]_0$ = 2.0 mM). Only 68% of the monomer was consumed in THF within 30 min, the slow reaction rate can be attributed to the competitive coordination of THF to inhibit the coordination of lactide to $K^+$ (Table 1, entry 1). All complexes show high activities (Table 1, entries 3−9) with toluene as the solvent. The sequence of activities is **3** > **2** > **1** for the three similar potassium complexes (Table 1, entries 2−4), which suggests the electron-donating group can accelerate the ROP reaction. In other words, the more negatively charged phenoxy anion is more active. Compared with complex **2**, the low


DOI: 10.1021/acs.inorgchem.5b02709
*Inorg. Chem.* XXXX, XXX, XXX−XXX

**Table 1. *rac*-Lactide Polymerization Catalyzed by 1−8[a]**

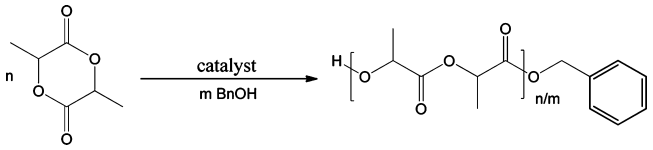


| entry | cat. | $[cat.]_0/[rac\text{-}LA]_0/[BnOH]_0$ | $t$ (min) | conversion[b] (%) | $M_{n,obsd}$[c] (g/mol) | $M_{n,calcd}$[d] (g/mol) | PDI | $P_m$[e] |
|---|---|---|---|---|---|---|---|---|
| 1[f] | **1** | 1/100/1 | 30 | 68 | 7200 | 9900 | 1.12 | 0.70 |
| 2 | **1** | 1/100/1 | 2 | 93 | 12800 | 13500 | 1.11 | 0.72 |
| 3 | **2** | 1/100/1 | 2 | 99 | 11600 | 14400 | 1.12 | 0.73 |
| 4 | **3** | 1/100/1 | 1.5 | 99 | 13500 | 14400 | 1.11 | 0.65 |
| 5 | **4** | 1/100/1 | 5 | 99 | 14400 | 14400 | 1.14 | 0.72 |
| 6 | **5** | 1/100/1 | 3 | 99 | 17200 | 14400 | 1.22 | 0.67 |
| 7 | **6** | 1/100/1 | 2 | 85 | 12700 | 12300 | 1.15 | 0.66 |
| 8 | **7** | 1/100/1 | 2 | 92 | 13300 | 13400 | 1.19 | 0.64 |
| 9 | **8** | 1/100/1 | 5 | 99 | 14100 | 14400 | 1.35 | 0.67 |
| 10 | **1** | 1/20/1 | 2 | 95 | 2500 | 2800 | 1.19 | 0.71 |
| 11 | **1** | 1/200/1 | 3 | 92 | 26600 | 26600 | 1.12 | 0.73 |
| 12 | **1** | 1/300/1 | 3 | 93 | 39400 | 40300 | 1.10 | 0.74 |
| 13 | **1** | 1/400/1 | 3 | 96 | 53100 | 55400 | 1.03 | 0.75 |
| 14[g] | **1** | 1/1000/50 | 3 | 99 | 2600 | 3000 | 1.08 | 0.70 |
| 15 | **1** | 1/20/0 | 2 | 96 | 14900 | 2800 | 1.39 | 0.70 |
| 16 | **1** | 1/50/0 | 2 | 94 | 18600 | 6800 | 1.46 | 0.71 |
| 17 | **1** | 1/100/0 | 2 | 92 (96)[h] | 12600 (19000)[h] | 13400 (13800)[h] | 1.44 (1.30)[h] | 0.71 (0.72)[h] |

[a]Conditions: reaction carried out under a dry nitrogen atmosphere, 0.01 mmol of catalyst, 5 mL of toluene, at room temperature, in addition to the annotated conditions. [b]Determined by $^1$H NMR spectroscopy. [c]Experimental $M_n$ and PDI determined by GPC in THF against polystyrene standards and corrected using the factor 0.58.[18] [d]Calculated from the molecular weight of *rac*-LA × $[LA]_0/[BnOH]_0$ × conversion yield + $M_{BnOH}$. [e]Determined by analysis of all of the tetrad signals in the methine region of the homonuclear-decoupled $^1$H NMR spectrum.[7,13] [f]In THF. [g]In 10 mL of toluene. [h]The data in parentheses were obtained from parallel experiments.

**Table 2. *rac*-Lactide Polymerization Catalyzed by 1−8 at −70 °C[a]**

| entry | cat. | $[cat.]_0/[rac\text{-}LA]_0/[BnOH]_0$ | $t$ (h) | conversion[b] (%) | $M_{n,obsd}$[c] (g/mol) | $M_{n,calcd}$[d] (g/mol) | PDI | $P_m$[e] | $T_m$[f] (°C) |
|---|---|---|---|---|---|---|---|---|---|
| 1 | **1** | 1/20/1 | 10 | 92 | 2300 | 2800 | 1.09 | 0.89 | 185.2 |
| 2[g] | **1** | 1/100/1 | 8 | 92 | 12300 | 13400 | 1.06 | 0.90 | 186.3 |
| 3 | **1** | 1/100/1 | 10 | 90 | 12000 | 13100 | 1.05 | 0.92 | 190.4 |
| 4 | **1** | 1/200/1 | 16 | 93 | 26500 | 26900 | 1.05 | 0.94 | 192.5 |
| 5 | **2** | 1/100/1 | 6 | 94 | 14000 | 13600 | 1.07 | 0.88 | 184.9 |
| 6 | **3** | 1/100/1 | 4 | 94 | 15200 | 13600 | 1.04 | 0.91 | 189.4 |
| 7 | **4** | 1/100/1 | 12 | 96 | 11300 | 14000 | 1.09 | 0.89 | 185.5 |
| 8 | **5** | 1/100/1 | 18 | 92 | 12500 | 13400 | 1.05 | 0.86 | 167.7 |
| 9 | **6** | 1/100/1 | 12 | 86 | 12000 | 12500 | 1.06 | 0.85 | 161.3 |
| 10 | **7** | 1/100/1 | 8 | 77 | 10300 | 11200 | 1.09 | 0.82 | (155.4) |
| 11 | **8** | 1/100/1 | 20 | 95 | 13900 | 13800 | 1.05 | 0.81 | (151.6) |

[a]Conditions: reactions carried out under a dry nitrogen atmosphere, 0.01 mmol of catalyst, 5 mL of toluene, at −70 °C, in addition to the annotated conditions. [b]Determined by $^1$H NMR spectroscopy. [c]Experimental $M_n$ and PDI determined by GPC in THF against polystyrene standards and corrected using the factor 0.58.[18] [d]Calculated from the molecular weight of *rac*-LA × $[LA]_0/[BnOH]_0$ × conversion yield + $M_{BnOH}$. [e]Determined by analysis of all of the tetrad signals in the methine region of the homonuclear-decoupled $^1$H NMR spectrum.[7,13] [f]Measured by DSC. $T_m$ values were recorded in the second run. The data in parentheses were obtained in the first run because the $T_m$ could not be detected in the second run due to slow crystallization. [g]At −60 °C.

activity of complex **4** illustrates the bulky *tert*-butyl group at another *ortho* position will slightly hinder the incoming lactide and decrease the ROP reaction rate (Table 1, entry 5). The same trend can also be found in the sodium analogues **5**−**8** (Table 1, entries 6−9). Compared to potassium complexes **1**−**4**, sodium complexes **5**−**8** are slightly less active. The environment around the sodium ion is more crowded than that around the potassium ion in complexes **1**−**4** for the smaller sodium ion radius. Consequently, the transport of lactide or BnOH to the active center will be slightly difficult in the sodium complexes. On the other hand, the oxyen of the phenoxy anion in the sodium complexes is less negatively charged because the Na−O bond is less ionic than the K−O bond, which can also lead to sodium complexes being less active. This trend is similar to that of other analogous sodium and potassium complexes.[11b,c] The polymerizations catalyzed by complexes **1**−**8** are living, which can be proved by the controllable molecular weights and low molecular weight distributions (Table 1, entries 1−9) and can be confirmed further by the fact that the molecular weights of polymers with complex **1** as a catalyst have a linear relationship with the ratio of $[rac\text{-}LA]_0$ to $[BnOH]_0$ (Table 1, entries 2 and 10−13, Figure S1). Complex **1** also can catalyze the immortal ROP of 1000 equiv of *rac*-lactide in the presence of 50 equiv of external



DOI: 10.1021/acs.inorgchem.5b02709
*Inorg. Chem.* XXXX, XXX, XXX−XXX

BnOH as a co-initiator, affording a controlled molecular weight and a relatively narrow PDI (Table 1, entry 14). In the absence of a co-initiator of BnOH, the ROP of *rac*-LA still proceeds quickly, but the molecular weights are not under control and the polydispersity is high (Table 1, entries 15−17).

**Stereoselectivity of the ROP of *rac*-Lactide, Structure Influences of the Catalysts, and Microstructure of Poly(*rac*-lactide).** As shown in Table 1, modest isoselective $P_m$ values ranging from 0.64 to 0.75 for complexes **1**−**8** can be achieved at room temperature in toluene, which are higher than the $P_m$ value of 0.55 for a similar potassium crown ether complex supported with a simple 2,4-di-*tert*-butylphenol ligand (Table S1, entry 1). Compared with THF, toluene is chosen as the solvent because a higher activity can be obtained in toluene using complex **1** as a catalyst, which can allow us to study the catalytic behavior at low temperature (Table 1, entries 1 and 2). The isoselectivities of potassium complexes are better than those of sodium complexes at room temperature possibly because the confined space of the sodium complexes is smaller due to the smaller plane of 15-crown-5 than 18-crown-6. The isoselectivities of complexes **1**, **2**, and **4** are similar, and the $P_m$ value of 0.65 for complex **3** is the lowest one in the four potassium complexes. Compared to those of complexes **1**, **2**, and **4**, the ROP reaction is very quick for complex **3** due to the strong electron-donating ability of the methoxy group, which hints that the energy barrier of ROP is very low.

With an attempt to improve the isoselectivity of the ROP of *rac*-lactide, we decreased the reaction temperature to −70 °C, and the reaction rate decreased remarkably. All polymers obtained are isotactically enriched with enhanced $P_m$ values of 0.88−0.94 when using potassium complexes **1**−**4** as the catalysts (Table 2, entries 1−7). The isoselectivity of complex **3** becomes similar to those of other potassium complexes. The *o*-*tert*-butyl group in complex **4** initially was designed to sandwich the active center well to increase the isoselectivity; however, compared to the similar complex **2**, the catalytic result sees no remarkable increase in the isoselectivity. This indicates that the effect of the *tert*-butyl group at the *ortho* position is not significant enough to increase the isoselectivity and the high isoselectivity mostly results from the sandwich structure constructed by the plane of the crown and the plane of the anthryl group. The simple potassium crown ether complex supported with a simple 2,4-di-*tert*-butylphenol ligand also exhibited a high isoselectivity of $P_m$ = 0.83 at −70 °C (Table S1, entry 2), which clearly indicates the sandwich structure is vital in this system again. However, the almost atactic polymers with $P_m$ = 0.55 obtained at room temperature (Table S1, entry 1) suggest the steric hindrance provided by the substituted group at the *ortho* position is also important. The isoselectivity of $P_m$ = 0.90 for complex **1** is better than $P_m$ = 0.86 for potassium complex **A** in Chart 1 at −60 °C under the same conditions (Table 2, entry 2). What is more, because the surroundings of the active center are too crowded, the ROP of lactide cannot proceed at room temperature with complex **A** as a catalyst, while complexes **1**−**8** can overcome the anti-Arrhenius behavior of potassium complex **A**.[11a] In addition, changing the previous bent xanthenyl plane to a standard planar substituted group of anthryl, the active center is sandwiched well and the high activity, which was sacrificed in systems **B** and **C** (Chart 1), is reserved even at −70 °C.[11b,c] The isoselectivities of sodium complexes **5**−**8** also increased sharply to above 0.80, although the $P_m$ values are still lower than those of the potassium analogues, the same as the trend at room temperature. All the above catalytic results show that the activity and isoselectivity of these types of potassium/sodium complexes are sensitive to the subtle confined space between the crown ether and the planar anthryl group. A best $P_m$ value of 0.94 was achieved (Table 2, entry 4) for complex **1** when the ratio $[rac\text{-LA}]_0/[\mathbf{1}]_0/[\text{BnOH}]_0$ was 200/1/1. This value is the highest recorded for alkali-metal complexes until now, which means this system is essentially comparable to the good Salen−Al system.

Typical $^1$H NMR, $^{13}$C NMR, and homonuclear-decoupled spectra of the methine region of poly(*rac*-lactide) [poly(*rac*-LA)] using **1** as a catalyst are shown in Figure 2A and Figure S2 (Table 2, entry 4).[7,13] The high isotacticities of the polymer can also be confirmed by high melting points as shown in Table 2; for example, the polymer with an isotacity of $P_m$ = 0.94 demonstrates a high $T_m$ of 192.5 °C (Figure 2B). It should be noted that the $P_m$ value determined from $^{13}$C NMR for this

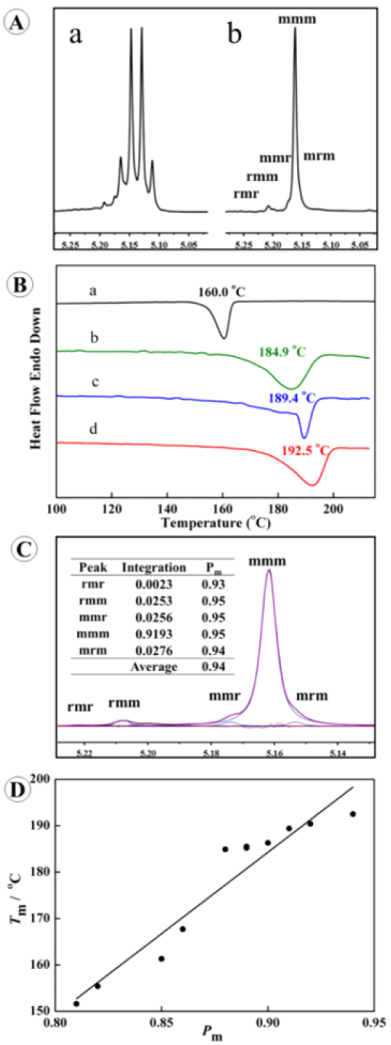


**Figure 2.** Characterization of poly(*rac*-lactide) by (A) the methine region of the (a) $^1$H NMR spectrum and (b) homonuclear-decoupled $^1$H NMR spectrum (Table 2, entry 4)[7,13] and (B) DSC thermograms of the second heating cycles of the samples of PLLA and poly(*rac*-lactide)s with different $P_m$ values [(a) PLLA, (b) $P_m$ = 0.88 (Table 2, entry 5), (c) $P_m$ = 0.91 (Table 2, entry 6), (d) $P_m$ = 0.94 (Table 2, entry 4)]. (C) $P_m$ values determined for all tetrads on the basis of Bernoulli statistics. Their average values were used (Table 2, entry 4). (D) Relationship between the $P_m$ values and the melting points.


DOI: 10.1021/acs.inorgchem.5b02709
*Inorg. Chem.* XXXX, XXX, XXX−XXX

sample is 0.92, which is comparable to the result from the determination by homonuclear-decoupled $^1$H NMR. The stereoerrors in the microscopic structure of a final polymer with a $P_m$ of 0.94 were analyzed by the tetrad signals in the homonuclear-decoupled $^1$H NMR spectrum (Table 2, entry 4; Figure 2C).[6q,8,11c] The signal intensity ratio of rmr, rmm, mmr, and mrm tetrad peaks was about 1/11/11/12. The isoslectivity calculation was based on the Bernoullian statistics of tetrads according to refs 6e, 6q, 13c, and 14. The theoretical ratios between these four tetrad peaks are close to the experimetal values. For example, the experimental value of [rmr]/[mrm] = 1/12 (8.3%) agrees well with the value of [rmr]/[mrm] = $[(1 - P_m)^2/2]/[(1 - P_m)/2] = 1 - P_m$ (8%) obtained from the $^{13}$C NMR determination and is also very close to the $1 - P_m$ value obtained from $^1$H NMR determination. Therefore, the isoselective mechanism of this system can be considered as a chain end control mechanism.[15] It should be noted that the high $T_m$ values accord well with the empirical function relationship between the isotacticity and melting temperature of the multiblock stereocopolymer of poly(*rac*-lactide) reported by Nomura et al. (Figure 2D),[16] which also can prove that the chain end control stereoselective mechanism is suitable for this system. Both the microscopic structure and the typical high $T_m$ values hint that these final poly(*rac*-lactide)s are multiblock stereocopolymers. The calculation based on the best isotacticity of $P_m$ = 0.94 suggests the average isotactic length can reach 15 (30 lactic acid units).[16]

End group analysis of the final polymer by $^1$H NMR spectroscopy revealed that all polymer chains are end-capped by one benzyl ester and a hydroxyl (Table 2, entry 1; Figure S3). The ESI mass spectrum of a final polymer (Table 2, entry 1; Figure S4) confirmed this further by a series of peaks at $144m + 108 + 18$ with a charge of +1, which can be assigned to $m(C_6H_8O_4)$ + BnOH + $NH_4^+$. It should be noted that there is another series of peaks at $0.5(144m + 108 + 18 + 18)$ with a charge of +2, which can be attributed to $m(C_6H_8O_4)$ + BnOH + $NH_4^+$ + $NH_4^+$. Both series of peaks with a difference in molecular mass of ∼144 Da suggest no serious trans-esterification reaction happens during this polymerization process. This information indicates that BnOH is a real initiator for the ROP of lactide. Therefore, as the monomer-activated mechanism is supposed for most alkali-metal phenoxides, the lactide can be activated after being coordinated to $K^+$ or $Na^+$, and consequently, the activated BnOH can attack the carbonyl group to initiate the ROP reaction.[10h,j] However, in this mechanism the role of the phenoxy is not well explained. Another ligand-assisted monomer-activated mechanism proposed by Davidson et al. in sodium aryloxide complex systems[10e] and Carpentier et al. in rare-earth-metal and alkaline-earth-metal cationic complex systems[17] seems to be suitable for this system because we found that the ROP reaction rate and stereoselectivity is highly related to the metal ion and phenoxy structure. For example, the electron-donating groups can remarkably increase the ROP reaction rate. It is reasonably explained that the phenoxy with an electron-donating group is more basic and more easily actives an alcohol via a hydrogen bond to accelerate the ROP reaction. The immortal ROP results also match this mechanism well. It should be noted that, in the absence of BnOH, no end groups were observed in the $^1$HNMR spectrum of the resultant PLA (Figure S5; Table 1, entry 16). The MALDI-TOF experiment suggested the polymer (Table 1, entry 16) is cyclic polylactide (Figure S6). This phenomenon has been reported and explained by Tabernero and Cano et al.[10k] These results suggest that the mechanism in the absence of an alcohol should be different from the reaction in the presence of alcohol. As Tabernero and Cano et al. pointed out, in the absence of an alcohol, ROP proceeds via a coordination−insertion mechanisum, while the ligand-assisted monomer-activated mechanism is suitable for the controllable ROP reaction in the presence of BnOH.

## CONCLUSIONS

The highly isoselective and living polymerization of *rac*-LA giving isotactic multiblock poly(*rac*-LA) catalyzed by a series of sodium and potassium *o*-(9-anthryl)phenolates was reported in this work. The donating group in phenolate can clearly accelerate the ROP reaction. The high isoselectivities of these complexes mostly result from their sandwich structure constructed by the plane of the crown and the plane of the anthryl group. The best isotacticity of $P_m$ = 0.94 achieved here was the highest recorded value for alkali-metal complexes, which demonstrates that this system is comparable to that of known stereoselective aluminum, rare-earth-metal, and zinc catalysis systems. These catalyst structures presented a new catalyst design feature for the stereoselective polymerization of cyclic esters: associating a crown ether (dipole interaction) and a bulky phenoxide (ionic interaction) with a Lewis acidic monocation, $Na^+$ or $K^+$, and embedding the active center in a confined space. Considering sodium and potassium are innocuous, abundant elements in the human body, it is valuable to improve this system for the ROP of *rac*-lactide, and we believe this type of catalyst can potentially be applied in future industry after a suitable elevation of this system.

## EXPERIMENTAL SECTION

**General Considerations.** All syntheses and manipulations of air- and moisture-sensitive materials were performed under a dry nitrogen atmosphere using standard Schlenk techniques or in a glovebox. $^1$H NMR and $^{13}$C NMR spectra were recorded on a Varian Mercury Plus 300 MHz spectrometer, a JNM-ECS 400 MHz spectrometer, and a Varian INOVA 600 MHz spectrometer. $^1$H NMR chemical shifts are reported in parts per million versus residual protons in deuterated solvents as follows: $\delta$ 7.26 ppm for chloroform-*d*, $\delta$ 7.16 ppm for benzene-$d_6$, $\delta$ 2.08 ppm for toluene-$d_8$. $^{13}$C NMR chemical shifts are reported in parts per million versus residual $^{13}$C in the solvent: $\delta$ 77.0 ppm for chloroform-*d*, $\delta$ 128.06 ppm for benzene-$d_6$, $\delta$ 137.48 ppm for toluene-$d_8$. The elemental compositions of the complexes were measured using an Elemental Vario EL series CHN analyzer with the samples under a nitrogen atmosphere. The molecular weights ($M_n$ and $M_w$) and the molecular weight distributions ($M_w/M_n$) of the polymer samples were measured by gel permeation chromatography (GPC) at 25 °C using THF as a solvent, an eluent flow rate of 1 mL/min, and narrow polystyrene standards as reference samples. The measurements were performed using a Waters 1525 binary system that was equipped with a Waters 2414 RI detector using two Styragel columns ($10^2$−$10^6$ kg/mol). Each reported value was corrected using a factor of 0.58 for polylactide according to the literature.[18] Calorimetric measurements were conducted using a Sapphire DSC apparatus manufactured by PerkinElmer Instruments. Polymer samples (5.0 mg) were placed in aluminum pans and heated/cooled at a rate of 10 °C min$^{-1}$ under a nitrogen atmosphere. The previous thermal history of the samples was erased by heating them to 200 °C before cooling them to 0 °C. Measurements were performed between 30 and 220 °C. The melting temperatures were evaluated as the maxima of the melting endotherms. The ESI mass spectroscopic data were obtained using a Thermo Scientific Orbitrap Elite mass spectrometer (LTQ Orbitrap Elite). The MALDI-TOF mass spectroscopic data were obtained using $\alpha$-cyano-4-hydroxycinnamic acid as the matrix in a Bruker Daltonics, Inc. BIFLEX III MALDI-TOF mass spectrometer.


DOI: 10.1021/acs.inorgchem.5b02709
*Inorg. Chem.* XXXX, XXX, XXX−XXX

**Materials.** Toluene, THF, and hexane were dried by refluxing with sodium and benzophenone ketyl; the latter serves as an indicator. $CH_2Cl_2$ was distilled from $P_2O_5$. *rac*-LA was purchased from Daigang BIO Engineer Ltd. of China and was recrystallized from toluene three times. $CDCl_3$ was purchased from J&K Scientific, Ltd. in Beijing and was dried over activated molecular sieves. $KN(SiMe_3)_2$ and $NaN(SiMe_3)_2$ were purchased from J&K Scientific Ltd. and used as received. 18-Crown-6 and 15-crown-5 were purchased from local companies and were used as received.

**Syntheses.** *Synthesis of 2-(9-Anthryl)phenol ($H^1L$).* A sample of 2-bromophenol (1.88 g, 11 mmol) was dissolved in 80 mL of THF and cooled to −20 °C using a low-temperature reactor. Under a nitrogen atmosphere 22 mmol of $^n$BuLi (8.8 mL, 2.5 M hexane solution) was added. The solution became white and was slowly warmed to room temperature over the course of 2 h. To this solution was slowly added 11 mmol of anthrone (2.13 g dissolved in 100 mL of THF), and the yellow solution which formed was stirred overnight. The solution was hydrolyzed with 30 mL of 6 M HCl and stirred for 1 h. The mixture was extracted with diethyl ether. The organic layer was washed three times with 500 mL of water, dried with $MgSO_4$, and evaporated to dryness, affording a brown solid. This crude product was purified by column chromatography over silica gel ($CH_2Cl_2$/petroleum ether = 1/5), affording 0.96 g (32%) of 2-(9-anthryl)phenol as an off-white solid. $^1$H NMR (300 MHz, chloroform-*d*, 25 °C): $\delta$ 8.52 (s, Ar-*H*, 1H), 8.03 (d, $J$ = 8.4 Hz, Ar-*H*, 2H), 7.65 (d, $J$ = 8.7 Hz, Ar-*H*, 2H), 7.53−7.35 (m, Ar-*H*, 5H), 7.25 (dd, $J$ = 7.5, 1.8 Hz, Ar-*H*, 1H), 7.17−7.09 (m, Ar-*H*, 2H), 4.49 (s, −O*H*, 1H). $^{13}$C NMR (100 MHz, chloroform-*d*, 25 °C): $\delta$ 153.73, 132.12, 131.50, 130.79, 129.83, 129.63, 128.56, 127.96, 126.33, 126.01, 125.50, 123.95, 120.69, 115.70. Anal. Calcd for $C_{20}H_{14}O$: C, 88.33; H, 4.99. Found: C, 88.76; H, 5.22.

*Synthesis of 2-(9-Anthryl)-4-tert-butylphenol ($H^2L$).* According to the procedure described above for $H^1L$, 2-bromo-4-*tert*-butylphenol (1.14g, 5 mmol) was converted to 2-(9-anthryl)-4-*tert*-butylphenol as an off-white powder (0.62 g, 38%). $^1$H NMR (300 MHz, chloroform-*d*, 25 °C): $\delta$ 8.57 (s, Ar-*H*, 1H), 8.08 (d, $J$ = 8.4 Hz, Ar-*H*, 2H), 7.70 (d, $J$ = 8.9 Hz, Ar-*H*, 2H), 7.43−7. 57 (m, Ar-*H*, 3H), 7.42 (ddd, $J$ = 8.6, 6.5, 1.4 Hz, Ar-*H*, 2H), 7.27 (d, $J$ = 2.5 Hz, Ar-*H*, 1H), 7.09 (d, $J$ = 8.6 Hz, Ar-*H*, 1H), 4.37 (s, −O*H*, 1H), 1.34 (s, ArC($CH_3$)$_3$, 9H). $^{13}$C NMR (75 MHz, chloroform-*d*, 25 °C): $\delta$ 151.38, 143.40, 131.56, 130.82, 130.53, 129.03, 128.57, 127.78, 126.58, 126.26, 126.20, 125.47, 123.22, 115.04, 34.25, 31.62. Anal. Calcd for $C_{24}H_{22}O$: C, 88.66; H, 7.08. Found: C, 88.31; H, 6.79.

*Synthesis of 2-(9-Anthryl)-4-methoxyphenol ($H^3L$).* According to the procedure described above for $H^1L$, 2-bromo-4-methoxyphenol (1.01 g, 5 mmol) was converted to 2-(9-anthryl)-4-methoxyphenol as a light yellow powder (0.56 g, 37%). $^1$H NMR (300 MHz, chloroform-*d*, 25 °C): $\delta$ 8.54 (s, Ar-*H*, 1H), 8.05 (d, $J$ = 8.3 Hz, Ar-*H*, 2H), 7.70 (d, $J$ = 8.6 Hz, Ar-*H*, 2H), 7.48 (ddd, $J$ = 8.3, 6.5, 1.4 Hz, Ar-*H*, 2H), 7.41 (ddd, $J$ = 8.1, 6.5, 1.5 Hz, Ar-*H*, 2H), 7.09 (d, $J$ = 8.9 Hz, Ar-*H*, 1H), 7.02 (dd, $J$ = 8.9, 2.9 Hz, Ar-*H*, 1H), 6.81 (d, $J$ = 2.8 Hz, Ar-*H*, 1H), 4.21 (s, −O*H*, 1H), 3.77 (s, −OC$H_3$, 3H). $^{13}$C NMR (75 MHz, chloroform-*d*, 25 °C): $\delta$ 153.47, 147.79, 131.50, 130.64, 129.73, 128.57, 127.99, 126.38, 126.03, 125.52, 124.49, 116.54, 116.46, 115.65, 55.76. Anal. Calcd for $C_{20}H_{16}O$: C, 88.63; H, 5.10. Found: C, 83.98; H, 5.37.

*Synthesis of 2-(9-Anthryl)-4,6-di-tert-butylphenol ($H^4L$).* According to the procedure described above for $H^1L$, 2-bromo-4,6-di-*tert*-butylphenol (1.42 g, 5 mmol) was converted to 2-(9-anthryl)-4,6-di-*tert*-butylphenol as a pale brown powder (0.57 g, 30%). $^1$H NMR (300 MHz, chloroform-*d*, 25 °C): $\delta$ 8.52 (s, 1H), 8.02 (d, $J$ = 7.9 Hz, Ar-*H*, 2H), 7.71 (d, $J$ = 8.8 Hz, Ar-*H*, 2H), 7.51 (d, $J$ = 2.4 Hz, Ar-*H*, 1H), 7.45 (ddd, $J$ = 8.3, 6.6, 1.3 Hz, Ar-*H*, 2H), 7.39 (ddd, $J$ = 8.2, 6.6, 1.6 Hz, Ar-*H*, 2H), 7.11 (d, $J$ = 2.4 Hz, Ar-*H*, 1H), 4.54 (s, −O*H*, 1H), 1.50 (s, 9H, ArC($CH_3$)$_3$), 1.34 (s, 9H, ArC($CH_3$)$_3$). $^{13}$C NMR (100 MHz, chloroform-*d*, 25 °C): $\delta$ 149.91, 142.13, 135.36, 131.65, 131.10, 131.02, 128.58, 127.82, 126.50, 126.37, 126.27, 125.49, 123.81, 123.70, 35.17, 34.45, 31.77, 29.77. Anal. Calcd for $C_{28}H_{30}O$: C, 87.72; H, 7.68. Found: C, 87.91; H, 7.90.

*Synthesis of Complex **1**.* To a solution of $H^1L$ (0.270 g, 1.0 mmol) and 18-crown-6 ether (0.264 g, 1.0 mmol) in tetrahydrofuran (20 mL) was slowly added $KN(SiMe_3)_2$ (1.0 mL of a 1.00 M solution in THF, 1.0 mmol) at 0 °C under a nitrogen atmosphere. During this process, the colorless solution changed to red. After the solution was stirred for 4 h at room temperature, the red precipitate formed was separated by filtration. The solid residue was washed with 20 mL of hexane and dried in vacuo to give complex **1** as a red powder (0.438 g, 77%). Red crystals of **1** suitable for X-ray diffraction studies were obtained from a benzene solution at room temperature. $^1$H NMR (400 MHz, toluene-$d_8$, 25 °C): $\delta$ 8.52 (d, $J$ = 8.8 Hz, Ar-*H*, 1H), 8.10 (s, Ar-*H*, 1H), 7.81 (d, $J$ = 8.4 Hz, Ar-*H*, 2H), 7.51 (t, $J$ = 7.6 Hz, Ar-*H*, 1H), 7.33−7.22 (m, Ar-*H*, 3H), 7.21−7.10 (m, Ar-*H*, 3H), 6.71 (t, $J$ = 7.0 Hz, 1H), 2.92 (s, crown ether-*H*, 24H). $^{13}$C NMR (100 MHz, toluene-$d_8$, 50 °C): $\delta$ 132.91, 132.71, 132.06, 131.12, 129.93, 126.46, 123.63, 123.40, 121.08, 70.05. Anal. Calcd for $C_{32}H_{37}KO_7$: C, 67.37; H, 6.23. Found: C, 67.11; H, 6.51.

*Synthesis of Complex **2**.* According to the procedure described above for **1**, $H^2L$ (0.326 g, 1.0 mmol) was converted to complex **2** as a red brown powder (0.502 g, 80%). $^1$H NMR (300 MHz, benzene-$d_6$, 25 °C): $\delta$ 8.78 (d, $J$ = 8.5 Hz, Ar-*H*, 2H), 8.17 (s, Ar-*H*, 1H), 7.88 (d, $J$ = 9.5 Hz, Ar-*H*, 2H), 7.72 (dd, $J$ = 8.6, 2.9 Hz, Ar-*H*, 1H), 7.48 (d, $J$ = 2.9 Hz, Ar-*H*, 1H), 7.30 (ddd, $J$ = 8.3, 6.4, 1.4 Hz, Ar-*H*, 2H), 7.22 (ddd, $J$ = 8.6, 6.4, 1.5 Hz, Ar-*H*, 2H), 7.19 (s, Ar-*H*, 1H), 2.85 (s, crown ether-*H*, 24H), 1.50 (s, ArC($CH_3$)$_3$, 9H). $^{13}$C NMR (100 MHz, benzene-$d_6$, 50 °C): $\delta$ 132.75, 132.14, 131.39, 129.73, 126.39, 125.49, 124.86, 123.41, 120.35, 69.94, 33.93, 32.69. Anal. Calcd for $C_{36}H_{45}KO_7$: C, 68.89; H, 7.50. Found: C, 68.76; H, 7.21.

*Synthesis of Complex **3**.* According to the procedure described above for **1**, $H^3L$ (0.300 g, 1.0 mmol) was converted to complex **3** as a deep red powder (0.510 g, 85%). Clear red crystals of **3** suitable for X-ray diffraction studies were obtained from a toluene solution at room temperature. $^1$H NMR (300 MHz, benzene-$d_6$, 25 °C): $\delta$ 8.56 (d, $J$ = 8.4 Hz, Ar-*H*, 2H), 8.20 (s, Ar-*H*, 1H), 7.87 (d, $J$ = 8.0 Hz, Ar-*H*, 2H), 7.47−7.30 (m, Ar-*H*, 1H), 7.37−7.19 (m, Ar-*H*, 5H), 7.07 (d, $J$ = 2.8 Hz, Ar-*H*, 1H), 3.54 (s, −OC$H_3$, 3H), 2.99 (s, crown ether-*H*, 24H). $^{13}$C NMR (100 MHz, benzene-$d_6$, 50 °C): $\delta$ 132.53, 131.71, 130.38, 125.57, 125.05, 124.68, 124.20, 118.62, 116.78, 70.21, 56.24. Anal. Calcd for $C_{33}H_{39}KO_8$: C, 65.99; H, 6.60. Found: C, 65.76; H, 6.52.

*Synthesis of Complex **4**.* According to the procedure described above for **1**, $H^4L$ (0.382 g, 1.0 mmol) was converted to complex **4** as a deep red powder (0.455 g, 67%). Red crystals of **4** suitable for X-ray diffraction studies were obtained from a benzene solution at room temperature. Because of the poor solubility of **4**, the expected information on $^{13}$C NMR was not achieved. $^1$H NMR (300 MHz, benzene-$d_6$, 25 °C): $\delta$ 8.76 (d, $J$ = 8.7 Hz, Ar-*H*, 2H), 8.07 (s, Ar-*H*, 1H), 7.88 (d, $J$ = 2.9 Hz, Ar-*H*, 1H), 7.82 (d, $J$ = 7.6 Hz, Ar-*H*, 2H), 7.28 (d, $J$ = 2.9 Hz, Ar-*H*, 1H), 7.24 (ddd, $J$ = 8.2, 6.4, 1.4 Hz, Ar-*H*, 2H), 7.13−7.19 (m, Ar-*H*, 2H), 2.75 (s, crown ether-*H*, 24H), 2.02 (s, ArC($CH_3$)$_3$, 9H), 1.55 (s, ArC($CH_3$)$_3$, 9H). Anal. Calcd for $C_{40}H_{53}KO_7$: C, 70.48; H, 7.92. Found: C, 70.14; H, 7.80.

*Synthesis of Complex **5**.* According to the procedure described abuove for **1**, $H^1L$ (0.270 g, 1.0 mmol) was converted to give complex **5** as a brown powder (0.250 g, 49%). $^1$H NMR (300 MHz, benzene-$d_6$, 25 °C): $\delta$ 8.64 (dd, $J$ = 8.7, 1.2 Hz, 2H), 8.16 (s, Ar-*H*, 1H), 7.81−7.91 (m, Ar-*H*, 2H), 7.69 (ddd, $J$ = 8.2, 7.0, 2.0 Hz, Ar-*H*, 1H), 7.46 (dd, $J$ = 7.3, 2.0 Hz, Ar-*H*, 1H), 7.33 (dd, $J$ = 8.3, 1.2 Hz, Ar-*H*, 1H), 7.24−7.30 (m, Ar-*H*, 2H), 7.20 (d, $J$ = 1.4 Hz, Ar-*H*, 1H), 7.17−7.18 (m, Ar-*H*, 1H), 6.88 (td, $J$ = 7.2, 1.3 Hz, Ar-*H*, 1H), 2.76 (s, crown ether-*H*, 20H). $^{13}$C NMR (100 MHz, benzene-$d_6$, 50 °C): $\delta$ 132.90, 132.63, 131.97, 130.84, 129.91, 126.75, 124.92, 123.80, 123.68, 121.12, 68.94. Anal. Calcd for $C_{30}H_{33}NaO_6$: C, 70.12; H, 6.25. Found: C, 70.30; H, 6.49.

*Synthesis of Complex **6**.* According to the procedure described above for **1**, $H^2L$ (0.326 g, 1.0 mmol) was converted to complex **6** as a dark red powder (0.396 g, 70%). $^1$H NMR (300 MHz, benzene-$d_6$, 25 °C): $\delta$ 8.70 (d, $J$ = 8.9 Hz, Ar-*H*, 2H), 8.17 (s, Ar-*H*, 1H), 7.87 (d, $J$ = 8.5 Hz, Ar-*H*, 2H), 7.70 (d, $J$ = 10.6 Hz, Ar-*H*, 1H), 7.48 (d, $J$ = 2.7 Hz, Ar-*H*, 1H), 7.16−7.35 (m, Ar-*H*, 5H), 2.73 (s, crown ether-*H*, 20H), 1.48 (s, ArC($CH_3$)$_3$, 9H). $^{13}$C NMR (100 MHz, benzene-$d_6$, 50 °C): $\delta$ 132.68, 132.02, 131.06, 130.88, 129.83, 129.64, 128.52, 126.55, 126.37, 125.58, 125.14, 124.73, 123.95, 123.77, 123.54, 123.41, 120.57,


DOI: 10.1021/acs.inorgchem.5b02709
*Inorg. Chem.* XXXX, XXX, XXX−XXX

120.18, 69.26, 33.95, 32.69, 32.49. Anal. Calcd for $C_{34}H_{41}NaO_6$: C, 71.03; H, 7.12. Found: C, 71.51; H, 7.27.

*Synthesis of Complex* ***7***. According to the procedure described above for **1**, $H^3L$ (0.300 g, 1.0 mmol) was converted to give complex **7** as a red powder (0.385 g, 71%). $^1$H NMR (300 MHz, benzene-$d_6$, 25 °C): $\delta$ 8.61 (d, $J$ = 8.1 Hz, Ar-*H*, 2H), 8.17 (s, Ar-*H*, 1H), 7.87 (d, $J$ = 8.3 Hz, Ar-*H*, 2H), 7.38 (dd, $J$ = 8.8, 3.0 Hz, Ar-*H*, 1H), 7.24−7.34 (m, Ar-*H*, 3H), 7.21 (d, $J$ = 7.7 Hz, Ar-*H*, 2H), 7.10 (d, $J$ = 3.0 Hz, Ar-*H*, 1H), 3.57 (s, −OC*H*$_3$, 3H), 2.72 (s, crown ether-*H*, 20H). $^{13}$C NMR (100 MHz, benzene-$d_6$, 50 °C): $\delta$ 132.36, 131.52, 129.15, 127.76, 125.77, 125.24, 124.90, 119.65, 118.14, 116.38, 69.96, 55.81. Anal. Calcd for $C_{31}H_{35}NaO_7$: C, 67.86; H, 6.72. Found: C, 68.62; H, 6.50.

*Synthesis of Complex* ***8***. According to the procedure described above for **1**, $H^4L$ (0.382 g, 1.0 mmol) was converted to complex **8** as a red-brown powder (0.468 g, 78%). Clear brown crystals of **8** suitable for X-ray diffraction studies were obtained from a glycol dimethyl ether solution at room temperature. $^1$H NMR (300 MHz, benzene-$d_6$, 25 °C): $\delta$ 8.69 (d, $J$ = 8.7 Hz, 2H), 8.08 (s, Ar-*H*, 1H), 7.88 (d, $J$ = 2.8 Hz, Ar-*H*, 1H), 7.82 (d, $J$ = 8.4 Hz, Ar-*H*, 2H), 7.27 (d, $J$ = 2.8 Hz, Ar-*H*, 1H), 7.24 (ddd, $J$ = 8.2, 6.4, 1.3 Hz, Ar-*H*, 2H), 7.13 (dd, $J$ = 6.5, 1.4 Hz, Ar-*H*, 2H), 2.47−2.75 (m, crown ether-*H*, 20H), 2.01 (s, ArC(C*H*$_3$)$_3$), 9H), 1.54 (s, ArC(C*H*$_3$)$_3$), 9H). $^{13}$C NMR (100 MHz, benzene-$d_6$, 50 °C): $\delta$ 136.19, 132.86, 132.26, 131.57, 128.51, 126.23, 124.87, 123.36, 122.81, 68.61, 36.15, 34.26, 32.84, 30.74. Anal. Calcd for $C_{38}H_{49}NaO_6$: C, 72.97; H, 7.83. Found: C, 73.05; H, 7.91.

**General Procedure for Polymerization of *rac*-Lactide.** A typical polymerization procedure is illustrated by the synthesis of PLA ($[LA]_0/[cat.]_0/[BnOH]_0$ = 100/1/1; Table 1, entry 2). *rac*-Lactide (0.144 g, 1.0 mmol) was added to a toluene solution of **1** (0.0057 g, 0.01 mmol) and BnOH (0.1 mL, 0.01 mmol, 0.1 M in toluene). The solution then was then rapidly stirred at room temperature for 3 min and quenched by a few drops of water. The polymer was precipitated by adding hexane (20 mL). A white crystalline solid was obtained by recrystallization from a $CH_2Cl_2$/hexane mixed solvent and dried under vacuum. It should be noted that just partial lactide can be soluble in toluene at room temperature or at −70 °C, but the reaction solution becomes clear when the polymerization proceeds and the monomer can be wholly consumed.

**Crystallographic Studies.** The data were collected using a SuperNova (Dual) X-ray diffractometer equipped with a graphite-monochromated Cu/Mo K$\alpha$ radiation source ($\lambda$ = 1.54184/0.71073 Å). The structures were solved by direct methods using the Siemens SHELXL-97 program.[19] Non-hydrogen atoms were refined with anisotropic displacement parameters during the final cycles. All hydrogen atoms were placed by geometrical considerations and were added to the structure factor calculations. The crystal data and refinement results are summarized in Table S1.

## ■ ASSOCIATED CONTENT

### Supporting Information

The Supporting Information is available free of charge on the ACS Publications website at DOI: 10.1021/acs.inorgchem.5b02709.

Experimental details of the synthesis and characterization of all compounds $H^1L$−$H^4L$ and **1**−**8**, NMR spectra of complexes **1**−**8**, and description of the polymerization studies (PDF)

Crystallographic data for complex **1** with CCDC reference number 1404985 (CIF)

Crystallographic data for complex **3** with CCDC reference number 1404986 (CIF)

Crystallographic data for complex **4** with CCDC reference number 1404987 (CIF)

Crystallographic data for complex **8** with CCDC reference number 1404988 (CIF)

## ■ AUTHOR INFORMATION


### Corresponding Author

*E-mail: wujc@lzu.edu.cn.


### Notes

The authors declare no competing financial interest.

## ■ ACKNOWLEDGMENTS

Financial support from the National Natural Science Foundation of China (Grants 21271092, 21171078, and 21401161), the Science Foundation of Gansu Province of China (Grant 1308RJ2A121), the project for the National Basic Science Personnel Training Fund (Grant J1103307), and the ScGrid of the Supercomputing Center of the Chinese Academy of Sciences is gratefully acknowledged. We thank Dr. Qingfeng Wu at the Institute of Modern Physics Chinese Academy of Sciences for the MALDI-TOF mass measurement.

## ■ REFERENCES


(1) (a) Okamoto, Y.; Nakano, T. *Chem. Rev.* **1994**, *94*, 349−372. (b) Chen, E. Y. X. *Chem. Rev.* **2009**, *109*, 5157−5214. (c) Childers, M. I.; Longo, J. M.; Van Zee, N. J.; LaPointe, A. M.; Coates, G. W. *Chem. Rev.* **2014**, *114*, 8129−8152.

(2) (a) *Comprehensive Asymmetric Catalysis I-III*; Jacobsen, E. N., Pfaltz, A., Yamamoto, H., Eds.; Springer-Verlag: Berlin, Heidelberg, 1999. (b) *Catalytic Asymmetric Synthesis*, 3rd ed.; Ojima, I., Ed.; John Wiley & Sons, Inc.: New York, 2010. (c) *Stereoselective Polymerization with Single-Site Catalysts*; Baugh, L. S., Canich, J. A. M., Eds.; CRC Press/Taylor & Francis Group: Boca Raton, FL, London, New York, 2007.

(3) (a) Cram, D. J.; Sogah, G. D. Y. *J. Chem. Soc., Chem. Commun.* **1981**, 625−628. (b) Cram, D. J.; Sogah, D. Y. *J. Am. Chem. Soc.* **1985**, *107*, 8301−8302.

(4) (a) Chiellini, E.; Solaro, R. *Adv. Mater.* **1996**, *8*, 305−313. (b) Uhrich, K. E.; Cannizzaro, S. M.; Langer, R. S.; Shakesheff, K. M. *Chem. Rev.* **1999**, *99*, 3181−3198. (c) Place, E. S.; George, J. H.; Williams, C. K.; Stevens, M. M. *Chem. Soc. Rev.* **2009**, *38*, 1139−51.

(5) (a) Dechy-Cabaret, O.; Martin-Vaca, B.; Bourissou, D. *Chem. Rev.* **2004**, *104*, 6147−76. (b) Stanford, M. J.; Dove, A. P. *Chem. Soc. Rev.* **2010**, *39*, 486−94. (c) Thomas, C. M. *Chem. Soc. Rev.* **2010**, *39*, 165−173.

(6) (a) Spassky, N.; Wisniewski, M.; Pluta, C.; Le Borgne, A. *Macromol. Chem. Phys.* **1996**, *197*, 2627−2637. (b) Radano, C. P.; Baker, G. L.; Smith, M. R. *J. Am. Chem. Soc.* **2000**, *122*, 1552−1553. (c) Zhong, Z.; Dijkstra, P. J.; Feijen, J. *Angew. Chem., Int. Ed.* **2002**, *41*, 4510−4513. (d) Nomura, N.; Ishii, R.; Akakura, M.; Aoi, K. *J. Am. Chem. Soc.* **2002**, *124*, 5938−5939. (e) Ovitt, T. M.; Coates, G. W. *J. Am. Chem. Soc.* **2002**, *124*, 1316−1326. (f) Zhong, Z.; Dijkstra, P. J.; Feijen, J. *J. Am. Chem. Soc.* **2003**, *125*, 11291−11298. (g) Hormnirun, P.; Marshall, E. L.; Gibson, V. C.; White, A. J. P.; Williams, D. J. *J. Am. Chem. Soc.* **2004**, *126*, 2688−2689. (h) Du, H.; Pang, X.; Yu, H.; Zhuang, X.; Chen, X.; Cui, D.; Wang, X.; Jing, X. *Macromolecules* **2007**, *40*, 1904−1913. (i) Nomura, N.; Ishii, R.; Yamamoto, Y.; Kondo, T. *Chem. - Eur. J.* **2007**, *13*, 4433−4451. (j) Chisholm, M. H.; Gallucci, J. C.; Quisenberry, K. T.; Zhou, Z. *Inorg. Chem.* **2008**, *47*, 2613−2624. (k) Du, H.; Velders, A. H.; Dijkstra, P. J.; Sun, J.; Zhong, Z.; Chen, X.; Feijen, J. *Chem. - Eur. J.* **2009**, *15*, 9836−9845. (l) Alaaeddine, A.; Thomas, C. M.; Roisnel, T.; Carpentier, J.-F. *Organometallics* **2009**, *28*, 1469−1475. (m) Whitelaw, E. L.; Loraine, G.; Mahon, M. F.; Jones, M. D. *Dalton Trans.* **2011**, *40*, 11469−11473. (n) Darensbourg, D. J.; Karroonnirun, O.; Wilson, S. J. *Inorg. Chem.* **2011**, *50*, 6775−6787. (o) Chen, H.-L.; Dutta, S.; Huang, P.-Y.; Lin, C.-C. *Organometallics* **2012**, *31*, 2016−2025. (p) Normand, M.; Dorcet, V.; Kirillov, E.; Carpentier, J.-F. *Organometallics* **2013**, *32*, 1694−1709. (q) Pilone, A.; Press, K.; Goldberg, I.; Kol, M.; Mazzeo, M.; Lamberti, M. *J. Am. Chem. Soc.* **2014**, *136*, 2940−2943. (r) Maudoux, N.; Roisnel, T.; Dorcet, V.; Carpentier, J.-F.; Sarazin, Y. *Chem. - Eur. J.* **2014**, *20*, 6131−6147. (s) Meduri, A.; Fuoco, T.; Lamberti, M.; Pellecchia, C.;




DOI: 10.1021/acs.inorgchem.5b02709
*Inorg. Chem.* XXXX, XXX, XXX−XXX

Pappalardo, D. *Macromolecules* **2014**, *47*, 534−543. (t) Press, K.; Goldberg, I.; Kol, M. *Angew. Chem., Int. Ed.* **2015**, 14858−14861.
(7) Bakewell, C.; Cao, T.-P.-A.; Long, N.; Le Goff, X. F.; Auffrant, A.; Williams, C. K. *J. Am. Chem. Soc.* **2012**, *134*, 20577−20580.
(8) Abbina, S.; Du, G. *ACS Macro Lett.* **2014**, *3*, 689−692.
(9) (a) Arnold, P. L.; Buffet, J.-C.; Blaudeck, R. P.; Sujecki, S.; Blake, A. J.; Wilson, C. *Angew. Chem., Int. Ed.* **2008**, *47*, 6033−6036. (b) Buffet, J.-C.; Okuda, J.; Arnold, P. L. *Inorg. Chem.* **2010**, *49*, 419−426. (c) Whitelaw, E. L.; Davidson, M. G.; Jones, M. D. *Chem. Commun.* **2011**, *47*, 10004−10006. (d) Horeglad, P.; Szczepaniak, G.; Dranka, M.; Zachara, J. *Chem. Commun.* **2012**, *48*, 1171−1173. (e) Stopper, A.; Okuda, J.; Kol, M. *Macromolecules* **2012**, *45*, 698−704. (f) Horeglad, P.; Litwińska, A.; Żukowska, G. Z.; Kubicki, D.; Szczepaniak, G.; Dranka, M.; Zachara, J. *Appl. Organomet. Chem.* **2013**, *27*, 328−336. (g) Bakewell, C.; White, A. J. P.; Long, N. J.; Williams, C. K. *Angew. Chem., Int. Ed.* **2014**, *53*, 9226−9230. (h) Jones, M. D.; Hancock, S. L.; McKeown, P.; Schafer, P. M.; Buchard, A.; Thomas, L. H.; Mahon, M. F.; Lowe, J. P. *Chem. Commun.* **2014**, *50*, 15967−15970. (i) Mou, Z.; Liu, B.; Wang, M.; Xie, H.; Li, P.; Li, L.; Li, S.; Cui, D. *Chem. Commun.* **2014**, *50*, 11411−11414. (j) Wang, H.; Yang, Y.; Ma, H. *Macromolecules* **2014**, *47*, 7750−7764. (k) Jones, M. D.; Brady, L.; McKeown, P.; Buchard, A.; Schafer, P. M.; Thomas, L. H.; Mahon, M. F.; Woodman, T. J.; Lowe, J. P. *Chem. Sci.* **2015**, *6*, 5034−5039. (l) Aluthge, D. C.; Ahn, J. M.; Mehrkhodavandi, P. *Chem. Sci.* **2015**, *6*, 5284−5292. (m) Honrado, M.; Otero, A.; Fernández-Baeza, J.; Sánchez-Barba, L. F.; Garcés, A.; Lara-Sánchez, A.; Martínez-Ferrer, J.; Sobrino, S.; Rodríguez, A. M. *Organometallics* **2015**, *34*, 3196−3208.
(10) (a) Kurcok, P.; Penczek, J.; Franek, J.; Jedlinski, Z. *Macromolecules* **1992**, *25*, 2285−2289. (b) Wu, J.; Yu, T.; Chen, C.; Lin, C. *Coord. Chem. Rev.* **2006**, *250*, 602−626. (c) Chen, H.-Y.; Zhang, J.; Lin, C.-C.; Reibenspies, J. H.; Miller, S. A. *Green Chem.* **2007**, *9*, 1038−1040. (d) Peng, Y.-L.; Huang, Y.; Chuang, H.-J.; Kuo, C.-Y.; Lin, C.-C. *Polymer* **2010**, *51*, 4329−4335. (e) Calvo, B.; Davidson, M. G.; García-Vivó, D. *Inorg. Chem.* **2011**, *50*, 3589−3595. (f) Zhang, J.; Jian, C.; Gao, Y.; Wang, L.; Tang, N.; Wu, J. *Inorg. Chem.* **2012**, *51*, 13380−13389. (g) Lu, W.-Y.; Hsiao, M.-W.; Hsu, S. C. N.; Peng, W.-T.; Chang, Y.-J.; Tsou, Y.-C.; Wu, T.-Y.; Lai, Y.-C.; Chen, Y.; Chen, H.-Y. *Dalton Trans.* **2012**, *41*, 3659−3667. (h) Chen, H.-Y.; Mialon, L.; Abboud, K. A.; Miller, S. A. *Organometallics* **2012**, *31*, 5252−5261. (i) Rosca, S.-C.; Rosca, D.-A.; Dorcet, V.; Kozak, C. M.; Kerton, F. M.; Carpentier, J.-F.; Sarazin, Y. *Dalton Trans.* **2013**, *42*, 9361−9375. (j) Huang, Y.; Wang, W.; Lin, C.-C.; Blake, M. P.; Clark, L.; Schwarz, A. D.; Mountford, P. *Dalton Trans.* **2013**, *42*, 9313−9324. (k) García-Valle, F. M.; Estivill, R.; Gallegos, C.; Cuenca, T.; Mosquera, M. E. G.; Tabernero, V.; Cano, J. *Organometallics* **2015**, *34*, 477−487.
(11) (a) Zhang, J.; Xiong, J.; Sun, Y.; Tang, N.; Wu, J. *Macromolecules* **2014**, *47*, 7789−7796. (b) Xiong, J.; Zhang, J.; Sun, Y.; Dai, Z.; Pan, X.; Wu, J. *Inorg. Chem.* **2015**, *54*, 1737−1743. (c) Dai, Z.; Sun, Y.; Xiong, J.; Pan, X.; Wu, J. *ACS Macro Lett.* **2015**, *4*, 556−560.
(12) Riley, P. N.; Thorn, M. G.; Vilardo, J. S.; Lockwood, M. A.; Fanwick, P. E.; Rothwell, I. P. *Organometallics* **1999**, *18*, 3016−3024.
(13) The PLA stereochemistry was assessed by comparison of the tetrad resonances observed in the homonuclear-decoupled $^1$HNMR spectra with the values predicted by Bernoullian statistics. The resolution of the integrals for the peaks corresponding to the rmr, rmm, mmr, mmm, and mrm tetrads was improved using peak deconvolution methods. The $P_m$ values were determined for all five tetrads, and their average was used as the $P_m$ for the initiator. (a) Coudane, J.; Ustariz-Peyret, C.; Schwach, G.; Vert, M. *J. Polym. Sci., Part A: Polym. Chem.* **1997**, *35*, 1651−1658. (b) Chisholm, M. H.; Iyer, S. S.; McCollum, D. G.; Pagel, M.; Werner-Zwanziger, U. *Macromolecules* **1999**, *32*, 963−973. (c) Kasperczyk, J. E. *Macromolecules* **1995**, *28*, 3937−3939. (d) Thakur, K. A. M.; Kean, R. T.; Hall, E. S.; Kolstad, J. J.; Lindgren, T. A.; Doscotch, M. A.; Siepmann, J. I.; Munson, E. J. *Macromolecules* **1997**, *30*, 2422−2428.
(14) Cheng, M.; Attygalle, A. B.; Lobkovsky, E. B.; Coates, G. W. *J. Am. Chem. Soc.* **1999**, *121*, 11583−11584.
(15) (a) Nomura, N.; Ishii, R.; Akakura, M.; Aoi, K. *J. Am. Chem. Soc.* **2002**, *124*, 5938−5939. (b) Chisholm, M. H.; Patmore, N. J.; Zhou, Z. *Chem. Commun.* **2005**, 127−129.
(16) Nomura, N.; Hasegawa, J.; Ishii, R. *Macromolecules* **2009**, *42*, 4907−4909.
(17) Liu, B.; Roisnel, T.; Maron, L.; Carpentier, J.-F.; Sarazin, Y. *Chem. - Eur. J.* **2013**, *19*, 3986−3994.
(18) Save, M.; Schappacher, M.; Soum, A. *Macromol. Chem. Phys.* **2002**, *203*, 889−899.
(19) Sheldrick, G. M. *SHELXL-97*; University of Göttingen: Göttingen, Germany, 1996.


DOI: 10.1021/acs.inorgchem.5b02709
*Inorg. Chem.* XXXX, XXX, XXX−XXX